Intercalation of a manganese(II)-thiacalixarene luminescent complex in layered double hydroxides: synthesis and photophysical characterization

Niall O'Toole, Constance Lecourt, Yan Suffren, Francois Toche, Rodica Chiriac, Nicole Gilon, François Bessueille, Arnaud Brioude, Erwann Jeanneau, Dominique Luneau, et al.

Intercalation of a manganese(II)-thiacalixarene luminescent complex in layered double hydroxides: synthesis and photophysical characterizations.

by Niall O'Toole [a], Constance Lecourt [a], Yan Suffren [b], François Toche [a], Rodica Chiriac [a], Nicole Gilon [c], François Bessueille [c], Arnaud Brioude [a], Erwann Jeanneau [a], Dominique Luneau [a], Cédric Desroches* [a].

[a] Laboratoire des Multimatériaux et Interfaces (UMR 5615), Université Claude Bernard de Lyon 1, Campus de la Doua, 69622 Villeurbanne, France.

E-mail: cedric.desroches@univ-lyon1.fr

[b] Univ Rennes, INSA Rennes, CNRS, ISCR "Institut des Sciences Chimiques de Rennes", F-35000 Rennes, France.

[c] Institut des Sciences Analytiques, UMR5280 Université Lyon 1-CNRS, Université de Lyon, 69622, Villeurbanne, Cedex, France.

Abstract

Utilizing the osmotic swelling of Layered Double Hydroxides (LDHs, $[Mg_{1-x}Al_x(OH)_2]^{x+}(NO_3^-)_x$) in formamide, the anionic luminescent complex $[(ThiaSO_2)_2(Mn^{II})_4F]^-$ ($ThiaSO_2$ = *p-tert*-butylsulfonylcalixarene) is introduced between the positive layers, leading to a doping of LDH. In the recovered LDH layers, the hexagonal prism morphology of the precursor is well retained. The formula of the resulting compound $(Mg_{0.71}Al_{0.29}(OH)_2(NO_3)_{0.288}((ThiaSO_2)_2(Mn)_4F)_{0.002}(H_2O)_{0.5})$ (**1**) was determined by elemental and thermogravimetric analysis. The low doping rate is attributed to the low negative charge density (e/Å^2) of the complex. Basal spacing of 12.02 Å indicates that $[(ThiaSO_2)_2(Mn^{II})_4F]^-$ is

sandwiched across the width by positive LDH layers. The photophysical properties of the compound **1** were studied in the solid state. **1** presents luminescence properties upon UV excitation, with the emission maximum centered at 630 nm and 650 nm in the presence and the absence of atmospheric O_2, respectively. Photophysical studies have been carried out under different atmospheres and using various excitation wavelengths. The relationship of the extinction of emission with the presence of molecular oxygen is reported, and demonstrates the very high sensitivity of this compound to oxygen. Finally, incorporation of the luminescent complex within the LDH host allows for the O_2-sensitivity to remain similar to that observed in solution whilst avoiding photo-degradation, thereby opening perspectives for use in oxygen sensing or singlet oxygen generation.

Introduction

Harnessing energy, and in particular energy of the electromagnetic spectrum, is of enormous societal and scientific significance, and methods of incorporating photoactive species into functional materials must be studied and optimised. There are numerous ways and means for the creation of this type of functional material. One of them is the preparation of so-called hybrid materials composed of an organic part and an inorganic part, each with a specific functionality.[1]

For several years we have been working on the coordination chemistry of thiacalixarene. [2] One major result has been the discovery of the strong luminescence, emitted at approximately 600 nm (excitation at 350 nm), shown by tetra-nuclear clusters of Mn^{II} ions sandwiched between two *p-tert*-butylsulfonylcalixarene macrocycles ($ThiaSO_2$), of formula $[(ThiaSO_2)_2(Mn^{II})_4F]K$. The $ThiaSO_2$ ligands were found to play the role of antenna in inducing this luminescence. Spectroscopic studies have demonstrated that interactions between the cation and the anionic cluster $[(ThiaSO_2)_2(Mn^{II})_4F]^-$ have an influence on the luminescence

quenching by energy transfer from the excited complex to O_2. These studies have shown that when the anion-cation separation distance increases such that the coordination interaction disappears, the molecular system becomes extremely sensitive to oxygen.[2b] To further study and exploit this phenomenon, we envision the intercalation of the luminescent $[(ThiaSO_2)_2(Mn^{II})_4F]^-$ anionic complex into the interlayer space of inorganic positively charged layered double hydroxide (LDH) materials.[3] Layered double hydroxides (LDHs) are composed of positively charged metal hydroxide layers containing divalent and trivalent cations such as Mg^{2+} and Al^{3+} and interlayer anions. The general formula is $[M_{1-x}M'_x(OH)_2]^{x+}(A^{m-})_{x/m}\ nH_2O$, where **M** is the divalent metal, **M'** is the trivalent metal, **x** is the degree of substitution, **A** is an anion of charge **m**, and **n** is the number of interstitial water molecules found in the cell. LDHs are unusual in that most materials of this structural type contain negatively charged layers.[4] The practical applications of LDHs are as varied as the potential components of the material. $[Mg_{1-x}Al_x(OH)_2]^{x+}(A^{m-})_{x/m}\ nH_2O$ are ideal candidates for the inorganic matrix to host functional anions such as this luminescent manganese-thiacalixarene cluster anion (Figure 1). The anionic nature of this luminescent species allows it to act as the interlayer anion in an LDH, offering a simple route towards the creation of a luminescent hybrid material.

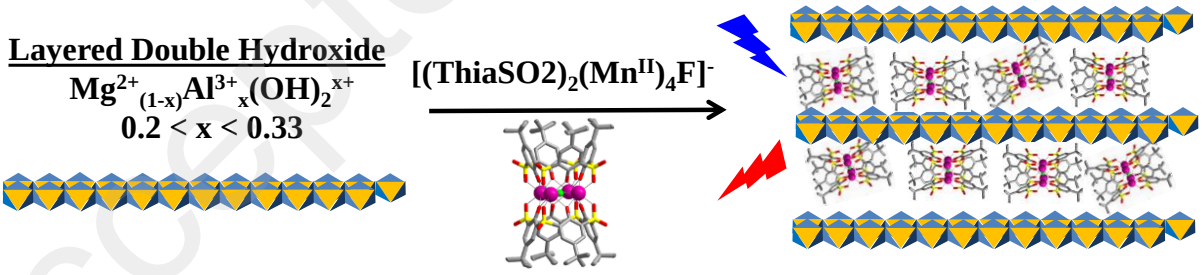

Figure 1: Schematic representation of $ThiaSO_2/Mn^{II}$ system intercalated in a layered double hydroxide.

The concept of photo-functional materials supported on host materials has gained considerable interest as a means of obtaining controllable optical properties for application in the next generation of light emitting materials and sensors.[5] Insertion of the $[(ThiaSO_2)_2(Mn)_4(F)]^-$ anion

between the positively charged hydroxide layers would allow us to evaluate the luminescence and oxygen sensibility shown by our system within such a matrix. The luminescence of these hybrid materials could also be modulated *via* various stimuli, such as pressure resulting from interlayer spacing and host-guest interactions. Insertion between the inorganic layers may also give rise to an ordered assemblage of the luminescent anions, allowing for materials demonstrating polarized photoemission properties.

In this paper, we report the synthesis and photophysical properties of LDHs materials doped with intercalated $[(ThiaSO_2)_2(Mn^{II})_4F]^-$ of formula $Mg_{0.71}Al_{0.29}(OH)_2(NO_3)_{0.288}((ThiaSO_2)_2(Mn)_4F)_{0.002}$ **1**. A red-orange luminescence is observed for compound **1** and has been attributed to luminescence of the complex sandwiched within the LDH, originating from the $^4T_1(t_{2g}^4e_g^1) \rightarrow {}^6A_1(t_{2g}^3e_g^2)$ d–d transition of the manganese(II) ions. We show the acute sensitivity of this luminescence to the presence of O_2, and conversely demonstrate that it remains stable to photo-oxidation, opening perspectives for its as application in oxygen sensing or singlet oxygen generation.

Results and discussion

Synthesis

Synthetic routes to LDH@[(ThiaSO$_2$)$_2$(Mn^{II})$_4$F] materials

Due to the insolubility of the luminescent $[(ThiaSO_2)_2(Mn^{II})_4F]K$ complex in most of the solvents compatible with the preparation of LDHs, we moved towards a two-step synthesis which consists of firstly preparing the LDH host matrix followed by an anion substitution to introduce our anionic complex. This second step, as described by Hibino,[6] makes use of the osmotic swelling of LDHs $[Mg_{1-x}Al_x(OH)_2]^{x+}(NO_3^-)_x$ in formamide and should allow insertion of the anionic luminescent $[(ThiaSO_2)_2(Mn^{II})_4F]^-$ complex ($ThiaSO_2$ = *p-tert*-butylsulfonylcalixarene) into the positive layers of LDHs.

There are many different synthetic methods towards LDHs, in part due to the incredible variety which is possible for this structural family. Hydrothermal synthesis seemed to us to be the most efficient. The reaction mixture consists of a salt, usually nitrate, of each desired metal (here $Mg(NO_3)_2$ and $Al(NO_3)_3$) and an amine which acts as an ammonia precursor compound.[7] The principle is that as the temperature increases, the amine is hydrolysed releasing ammonia into the solution thus raising the pH and bringing about the precipitation of the product. This method works better when the trivalent ion involved is aluminium; the amphoteric nature of the Al^{3+} ion makes it an effective centre for precipitation of the product in the fluctuating pH solution.[8] Thus, LDH Hydrotalcite (Mg-Al-CO_3 LDH) was synthesized by hydrothermal reaction of magnesium nitrate hexahydrate $Mg(NO_3)_2 \cdot 6H_2O$ and aluminium nitrate nonahydrate $Al(NO_3)_3 \cdot 9H_2O$, in the presence of hexamethylenetetramine (HMT, $C_6H_{12}N_4$), maintained at a temperature of 140°C for 24 hours. The resulting precipitate was recovered by centrifugation and washed with deionised water at least three times. Because of the strength of the attraction between the carbonate ion and the interlayer space of the LDH, this species is substituted with nitrate anions before the complex intercalation takes place.[9] To this end, the LDH-carbonate is suspended in an aqueous acid - salt solution of concentration 0.005 $mol.L^{-1}$ $NaNO_3$ and 1 $mol.L^{-1}$ HNO_3 under a neutral atmosphere (Ar or N_2). After stirring for 16 hours at room temperature, the product is recovered by centrifugation and washed with degassed water. From the nitrate material direct anion exchange with the anionic $[(ThiaSO_2)_2(Mn)_4F]^-$ cluster can be carried out. This entire process is done under inert atmosphere to avoid contamination with CO_2 from the surroundings, which would form carbonate anions within the LDH layers. First the LDH-nitrate is suspended in formamide (0.02 g in 50 cm^3 of formamide). Osmotic pressure of the formamide molecules pushes apart the LDH layers causing exfoliation, eventually leading to total dissociation. The resulting suspension shows Tyndall scattering when a beam of light is shone through it. A dimethylformamide solution of the luminescent complex (0.025 $mol.L^{-1}$)

is added to the LDH suspension, which immediately becomes cloudy as the hydroxide nano-sheets reform around the luminescent centres. Generally, for this type of procedure, the guest anion is dissolved in formamide. Unfortunately, our complex is insoluble in formamide; solubility has thus far only been observed in DMF or DMSO. Moreover, the solvent DMF on its own induces a tightening of the hydroxide layers. For these reasons a solution of complex in a minimum of DMF is prepared and added slowly. The intercalated product is the removed from suspension by centrifugation, washed with DMF and water several times and obtained as off-white micro-powder. Variations of temperature, agitation, order of addition and so on were attempted for this reaction, to optimise the conditions. The following is a generalised synthesis for these compounds derived from this optimisation: 24 h stirring time at 25°C seems to be the most effective parameters.

The formula $Mg_{0.71}Al_{0.29}(OH)_2(NO_3)_{0.288}((ThiaSO_2)_2(Mn)_4F)_{0.002}$ of **1** was obtained by elemental analysis and indicates that only a small amount of complex is embedded in LDH. Thus, we can consider the anionic layers of these materials to be constituted of mostly nitrate ions, with comparatively few anionic $[(ThiaSO_2)_2(Mn)_4F]^-$ cluster. LDHs exhibit a high positive charge density on the main layers. For example, a ratio of trivalent to divalent metal of x = 1/3 corresponds to one charge per 50 $Å^2$ on each side of the layer, leading to one charge for each 25 $Å^2$ in the inter-lamellar domains.[10] Our cluster complex represents one negative charge for each 170 $Å^2$. Thus, it is difficult to achieve electroneutrality with only these complexes inside the interlayer space. In the literature, the majority of calixarene derivatives inserted in LDH systems are sulfonated, with four negative charges per macrocycle.[11] Therefore, they have a higher negative charge density and can fully substitute nitrate ions. A similar case in the literature deals with a sulfonated thiacalixarene complex complexed with an Ag^+ ion. In this case, despite a head to tail arrangement of the macrocycles to increase the charge density per unit volume, the macrocycle layer is still supplemented by carbonate anions.[12]

On the basis of the charge density of the LDH layers and the molecular dimensions of $[(ThiaSO_2)_2(Mn^{II})_4F]^-$, we believe that the extent of intercalation is limited by the size of the complex and not by the LDH anion-exchange capacity. This phenomenon has already been encountered with low charge density molecular systems such as ruthenium-based complexes.[13]

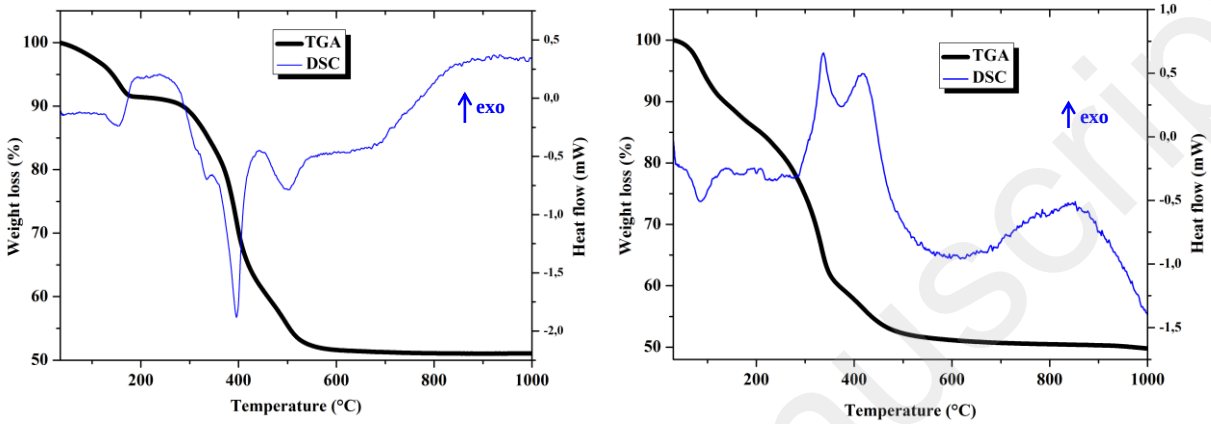

Figure 2: TGA (black curve) and DSC (blue curve) of Mg-Al-NO_3 LDHs (left) and LDH-complex (right).

The calculation of the mass losses from the TGA curves are in agreement with formulae $Mg_{0.72}Al_{0.28}(OH)_2(NO_3)_{0.28}(H_2O)_{0.36}$ for Mg-Al-NO_3 LDH and $Mg_{0.71}Al_{0.29}(OH)_2(NO_3)_{0.288}((ThiaSO_2)_2(Mn)_4F)_{0.002}(H_2O)_{0.5}$ for compound **1**, and are consistent with the formulae obtained from the elementary analysis (see Figures S1-S4 in Supporting Information).

Regarding the TGA curves, decomposition of LDHs occurred in three consequent steps. In Figure 2, the first step observed in the range of 50–200°C corresponds to solvent loss from internal gallery surfaces and the external non gallery surfaces. For Mg-Al-NO_3 LDH, the second step in the range of 200–400°C is mainly attributed to the dehydroxylation and the third step, observed above 400°C, arises due to the elimination of NO_3^- from the LDH interlayer space.[14] For **1**, the second and third steps resemble those of Mg-Al-NO_3 LDH and it is difficult to identify the loss of mass specifically due to the complex.

The DSC for Mg-Al-NO_3 LDH and compound **1** show three major peaks, the positions of which fit remarkably well with those in the DTG curve, indicating that they correspond to mass-loss processes. For Mg-Al-NO_3 LDH all peaks are endothermic, contrarily to the exothermic peaks of compound **1** which are attributed to decomposition (between 300 and 500°C). The complex has a basic formula of $C_{82}H_{96}FMn_4O_{26}S_8$, leading to a general formula for compound **1** of $Mg_{0.71}Al_{0.29}(OH)_2(NO_3)_{0.288}C_{0.16}H_{0.19}F_{0.002}Mn_{0.008}O_{0.05}S_{0.016}$. The oxidation of the organic part of the compound is very exothermic and explains the exothermicity of the peaks observed on the DSC curve for compound **1**.

X-Ray Diffraction Characterization

Figure 3 shows the powder X-Ray Diffraction diagram of intercalate material compared with the diagrams for carbonate and nitrate Mg-Al layered double hydroxides. the X-Ray Diffraction patterns of compounds Mg-Al-CO3 (red curve) and Mg-Al-NO3 (blue curve) shows that for each compound, the products were obtained in a pure phase. These patterns correspond to those described in the literature.[3, 6b)] We would expect to see peaks corresponding to the (003) and (006) planes as with the carbonate and nitrate forms, shifted to a lower 2θ value as a result of the larger size of the complex anion creating a larger interlayer space. For the sample intercalated product **1** (Figure 3, green curve), the diagram shows a succession of three broad peaks positioned at 7.34° (*d* = 12.02 Å), 14.96° (*d* = 5.91 Å) and 29.91 (*d* = 3.89 Å).

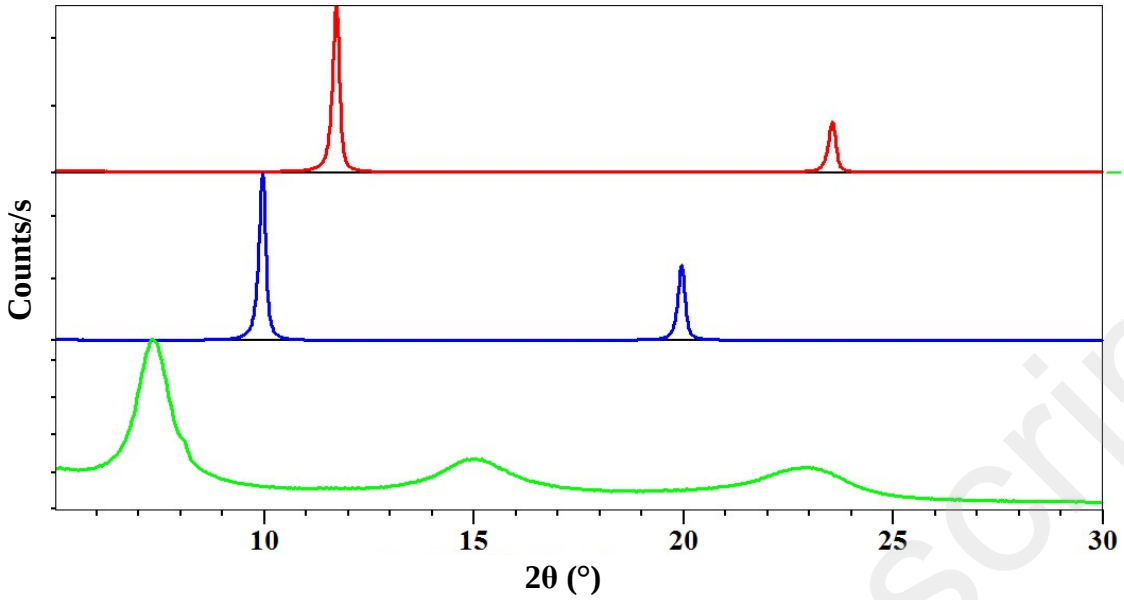

Figure 3: Powder X-Ray Diffraction patterns of Mg-Al-CO_3 (red pattern), Mg-Al-NO_3 (blue pattern) and product **1** (green pattern). The X-Ray patterns are obtained with an X-Ray source of λ = 1.54060 Å over an angular range from 2° to 30°.

The three peaks observed for compound **1** could not be indexed. The expected numerical relationships between *d* values are not exactly appropriate to make analogy with the inter-reticular distance indices d_{003}, d_{006} and d_{009} obtained for Mg-Al-NO_3 or Mg-Al-CO_3 systems. For example, we would expect the largest *d* value to correspond to the (003) plane, which would mean that the smaller distances would be exact divisions of this; 12.02 / 2 = 6.01 Å for the (006) plane, 12.02 / 3 = 4.00 Å for the (009). This is evidently not exactly the case. The peak forms are less sharp, with broader, less intense peaks than those seen for the nitrate and carbonate LDHs. This could be explained by the disorder introduced by the anion distribution within the LDH layers and/or by the size of fundamental crystallization domains. The crystal packing of $[(ThiaSO_2)_2(Mn)_4F]K$ shows that $[(ThiaSO_2)_2(Mn)_4F]^-$ anions are linked through the coordinated potassium ion and sulphonyl group, making $[(ThiaSO_2)_2(Mn)_4F]K$ a one-dimensional network with a distance between two cations of 12.1 Å (Figure 4). The charge balancing cation is found near the sulfonyl groups, in the plane

formed by the four manganese ions, indicating that the negative charge is concentrated in this region. The width of complex **1** is between 7.5 and 10.5 Å (see Figure S5 in Supporting Information) and a layer of Mg-Al hydroxide has a width of 4.8 Å.[15] The first observed distance derived from the X-Ray diagram, which is equal to 12.02 Å, could therefore correspond to the hypothesis presented in Figure 4 for which the anion $[(ThiaSO_2)_2(Mn)_4F]^-$ is sandwiched lengthwise by positive LDH layers.

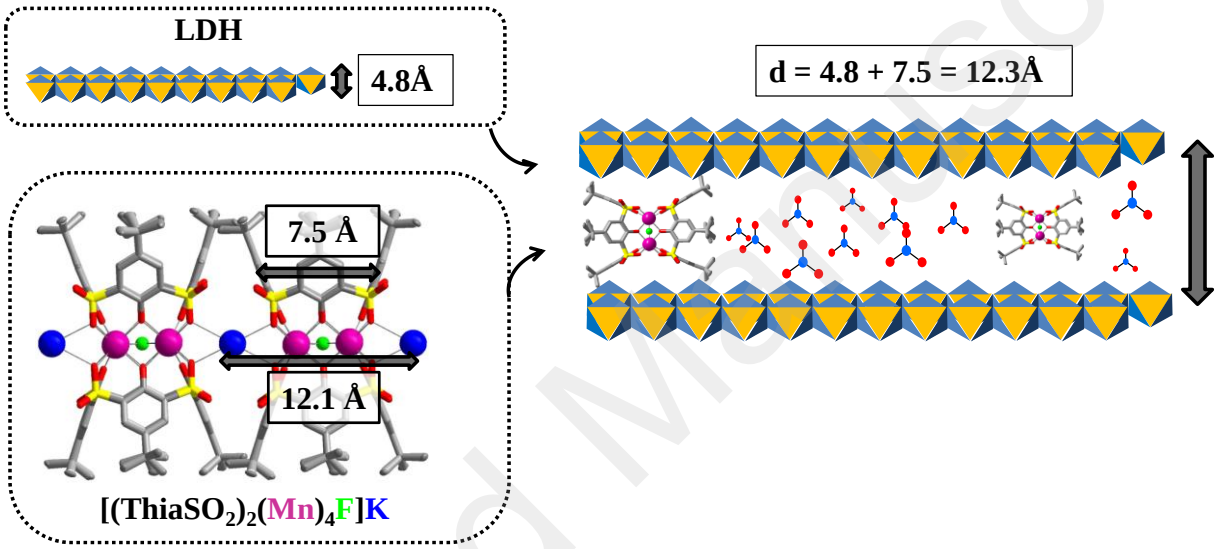

Figure 4: Schematic of hypothesised potential phases formed by the intercalation of luminescent aggregate into Mg-Al LDH.

Figure 5 shows a comparison of the X-Ray Diffraction data obtained for the LDH hybrid product obtained after a stirring time of 24 h (Product 1, green curve), and after a stirring time of 72 h (product 2, violet curve). While their X-ray diffraction diagrams are similar, the elementary analysis and spectroscopy characterizations show that these two compounds are different.

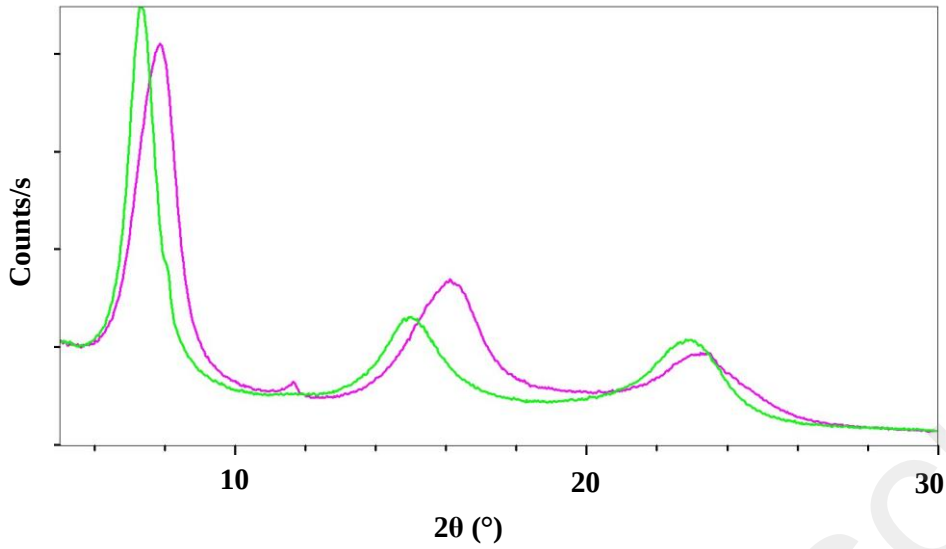

Figure 5: Overlay comparison of the X-Ray diffractograms obtained with an X-Ray source of λ = 1.54060 Å over an angular range from 2° to 30° of the intercalated hybrid material. The green curve corresponds to compound **1** and the violet curve corresponds to the compound **2** stirred for 72 h.

Elemental analysis has been run on LDH-NO_3 and the two compounds LDH-[$(ThiaSO_2)_2(Mn)_4F$]. The formulae found are $Mg_{0.72}Al_{0.28}(OH)_2(NO_3)_{0.28}$ for LDH-NO_3, $Mg_{0.71}Al_{0.29}(OH)_2(NO_3)_{0.288}((ThiaSO_2)_2(Mn)_4F)_{0.002}$ for compound **1** and $Mg_{0.57}Al_{0.43}(OH)_2(NO_3)_{0.425}((ThiaSO_2)_2(Mn)_4F)_{0.005}$ for compound **2**. The ratio Mg/Al is the same for LDH-NO_3 and compound **1**, but differs for compound **2**. It has been suggested that ion-exchange reactions at relatively low pH favour leaching of M^{II} ions from the layers, thus giving rise to higher values of x. It seems therefore that for compound **2**, and for all compounds which are subjected to long stirring duration with $[(ThiaSO_2)_2(Mn)_4F]^-$, the reaction conditions lead to leaching of Mg^{2+}. A possible hypothesis to explain this is a competition between the three metal ions, Mg^{2+}, Mn^{2+} and Al^{3+} for complexation with $ThiaSO_2$. It appears that under these synthesis conditions, the $ThiaSO_2$ ligands extricate Mg^{2+} ions from the inorganic hydroxide layers. Thus, the excess Al^{3+} seen in compound **2** is likely in the form of

oxo-hydroxide which is most probably amorphous and therefore not detected by XRD. To try to understand this hypothesis, we introduced to a DMF solution of a salt of either Mg^{2+} or Al^{3+} the $[(ThiaSO_2)_2(Mn)_4F]K$ complex.

In the case of Al^{3+} the reaction between $[(ThiaSO_2)_2(Mn)_4F]K$ and aluminium(III) nitrate nonahydrate in DMF at room temperature yielded white rectangular block crystals, which were studied by single crystal X-Ray Diffraction. Figure 6 shows the structure obtained from this analysis (see Figure S6 and crystallographic data in Tables S1-S3 in Supporting Information). The metal core consists of four Al^{3+} ions in an approximate square planar arrangement, linked by μ^2-hydroxide ligands lying in this metal plane. Most generally clusters with four aluminium ions, bridged by hydroxide ions, adopt a cubane-type structure. Here, the aluminium cluster architecture obtained for the $[Al_4(ThiaSO_2)_2]$ complex is uncommon, especially for aluminium ions displaying an octahedral coordination geometry.[16] Each metal centre shows identical pseudo-octahedral coordination geometry, with two bonds to hydroxide ligands, two bonds to phenolic oxygen from the thiacalixarene and one to a sulfonyl oxygen, with a molecule of DMF completing the coordination sphere.

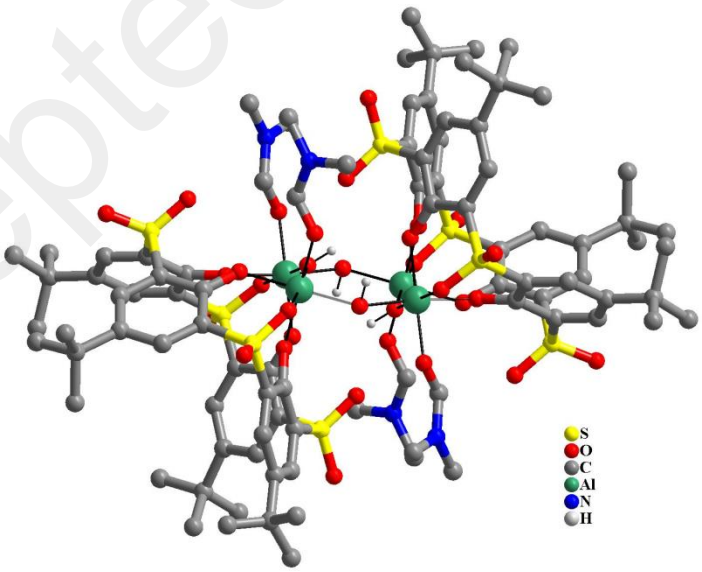

Figure 6: Structure of tetra-aluminium complex of $Al_4(ThiaSO_2)_2$. Color key: C = grey capped sticks, Al = green, S = yellow, O = red, N = blue.

Each ThiaSO_2 macrocycle coordinate two aluminium ions, in a rare hexadentate pinched cone conformation fashion, such that the angle formed by O – Al – O is approximately 90° for all coordinating oxygen atoms.

Scanning Electron Microscopy

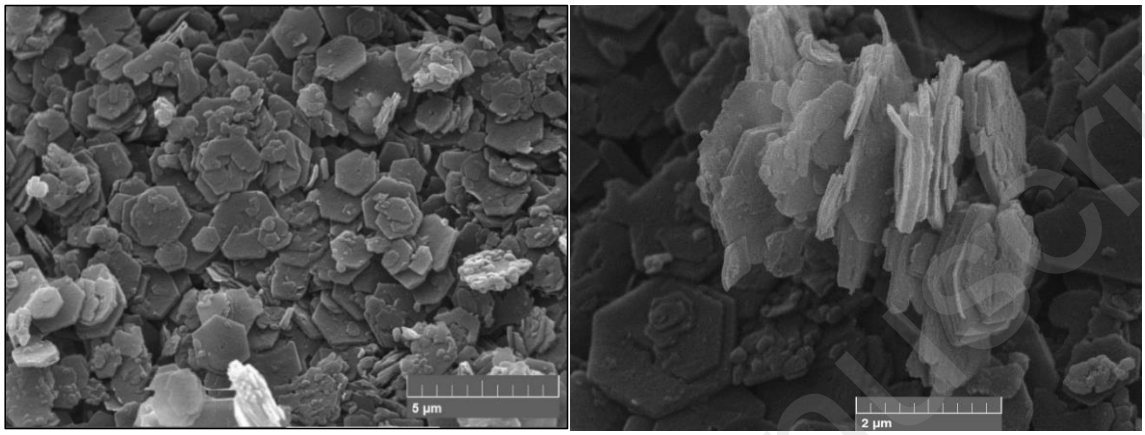

Figure 7: SEM images of intercalated LDH product **1**.

Hydrotalcite and its nitrate derivative both crystallize in the trigonal-rhombohedral (*R*-3*m*, n° 166) lattice system. The symmetry arising from this crystalline class results in a hexagonal form of the particles. Figure S7 (in Supporting Information) shows SEM images of the crystalline form of the nitrated material, proving that there has been no (or minimal) deformation during the acid-salt treatment (LDHs can be vulnerable to attack by strong acid). Figure 7 shows the hexagonal crystalline form for intercalated LDH **1** remains unchanged. We can therefore say that no major changes in terms of morphology (and by association therefore, perhaps in terms of symmetry class) have occurred.

Photophysical characterization of compound 1

The solid-state luminescence spectra have been recorded for compound **1** in the presence and absence of atmospheric O_2 (O_2 or N_2 atmosphere, respectively). Figure 8 shows the evolution of the excitation and emission spectra with respect to atmosphere. The solid-state excitation spectrum shows a UV band above 25000 cm^{-1} (below 400 nm) arising from the ligand-centered-absorption (π-π^* transitions). To avoid quenching by oxygen (O_2), the

luminescence was measured under N_2 atmosphere. The emission band maximum increased by around 400% and redshifted by -490 cm^{-1} (+20 nm) from 15870 cm^{-1} (630 nm) to 15380 cm^{-1} (650 nm) as shown in Figure 8. Successive emission measurements by changing atmospheres (N_2 and O_2) have revealed that the variation in luminescence intensity is reversible (schematized by the double arrow in figure 8). The study of this reversibility was again carried out on compound **1** after aging for one year under ambient atmosphere (Fig. S8). The same emission profile was observed, demonstrating the stability of this phenomenon over time.

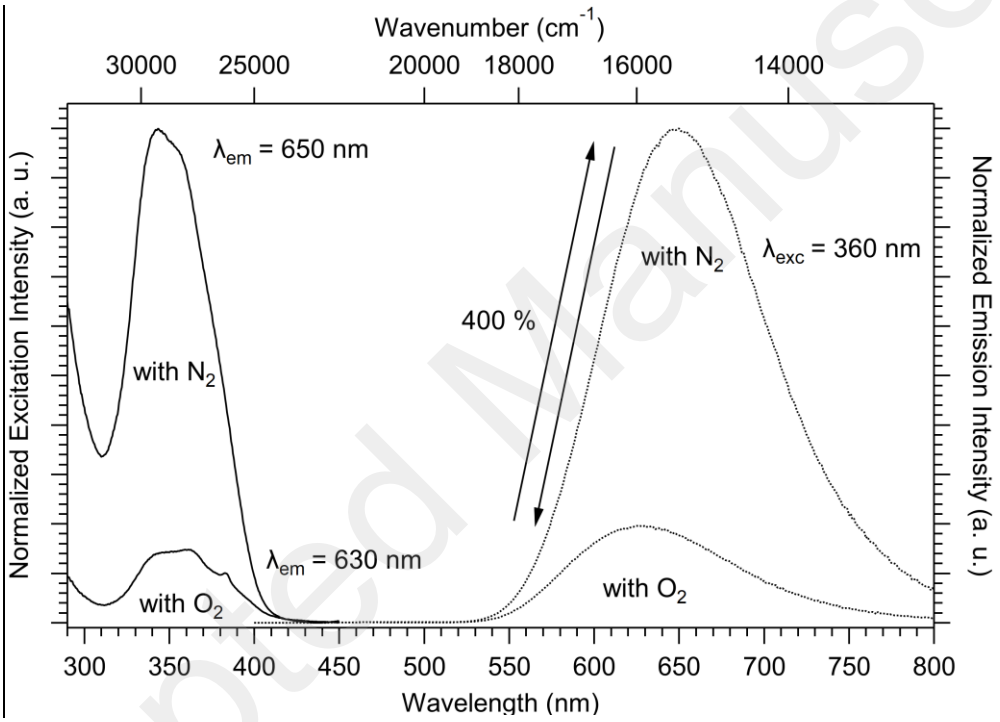

Figure 8: Solid-state normalized excitation (λ_{em} = 630 or 650 nm) and emission (λ_{ex} = 360 nm) spectra of **1** at 293 K with O_2 or N_2 atmosphere. τ_{obs} = 0.13(1) ms or 1.02(2) ms, with O_2 or N_2 atmosphere at 293 K, respectively. The double arrow represents the reversibility of the phenomenon.

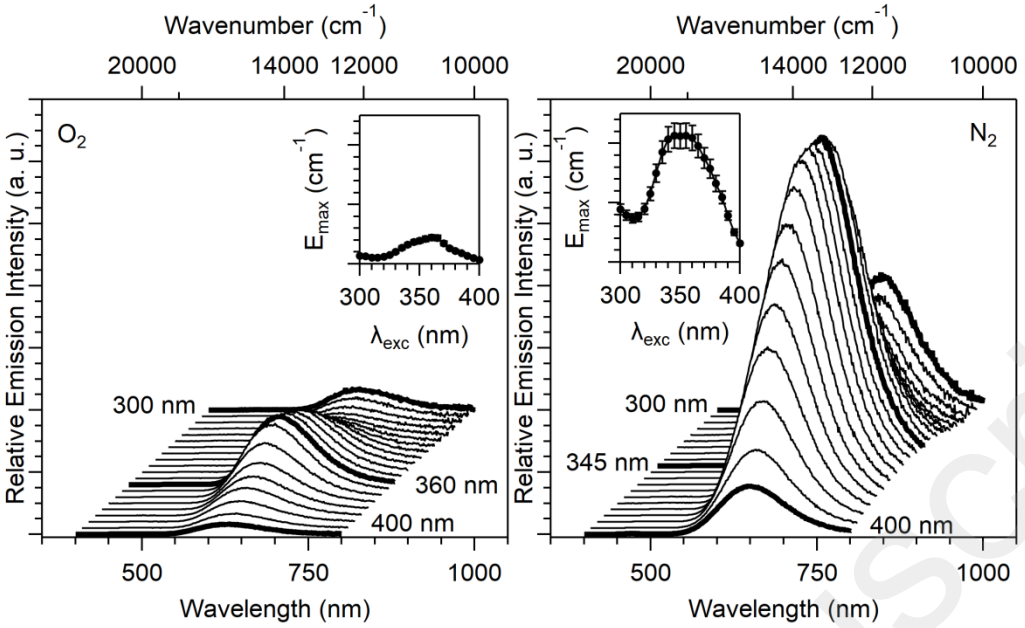

Figure 9. Solid-state relative emission spectra *vs* excitation wavelength (λ_{ex} = 300 - 400 nm) of **1** at 293 K with O_2 atmosphere (left) and N_2 atmosphere (right). The energy band maxima E_{max} *vs* excitation wavelength are plotted in insets. The two series of measurements with O_2 and N_2 are plotted with the same interval on the y-axis to highlight the enhancement factor of luminescence of **1** under N_2 atmosphere (≈ 400% upon photoexcitation at λ_{ex} = 360 nm). Error bars = 10%.

The emission spectra (λ_{em} = 25000 - 12500 cm^{-1} or 400 - 800 nm) have been measured at variable excitation wavelengths ranging between 33333 – 25000 cm^{-1} (λ_{exc} = 300 - 400 nm, Figure 9) under different atmospheres (N_2 and O_2). Under N_2 atmosphere, the emission spectra show a maximum band centered at 15380 cm^{-1} (650 nm), where spectra measured under an excitation of 340 - 365 nm showed the strongest emission intensity. Under O_2 atmosphere, emission spectra show a maximum band centered at 15870 cm^{-1} (630 nm), and the excitation range corresponding to the most intense emission spectra was between 355 - 365 nm. For the two sets of atmospheric parameters (N_2 and O_2), the emission band shows two maxima, one for

an excitation lower than 300 nm (this maximum cannot be precisely determined on our experimental setup) and a second around 360 nm.

The photophysical properties of **1** have been also studied at variable temperature between 77 K and 293 K (Figures S9 and S10), and the excitation and emission spectra were found to be slightly sensitive to changes in the temperature. In this temperature range, a weak redshift of the energy band maximum E_{max} of -340 cm^{-1} (+14 nm) from 15720 cm^{-1} to 15380 cm^{-1} (636 – 650 nm) and an increase of the band width at half height F_{WHM} of +330 cm^{-1} from 2350 cm^{-1} to 2680 cm^{-1} (+18 nm from 96 nm to 114 nm) of the broad band were observed. Vibronic intensity gains lead to a broadening of the luminescence band, a trend which is typical of d-d (metal centered) luminescence transitions such as for Mn^{2+}.[2b)] The lifetime under N_2 atmosphere at 77 K has been estimated at 1.51(1) ms compared to 1.02(2) ms at 293 K. This increase of 50% is due to a reduction of the non-radiative effects as the temperature decreases. Previous spectroscopic studies have demonstrated that an influence is exerted on this luminescence quenching (energy transfers from the excited complex to O_2) by interaction between the cation and the anionic cluster. These studies show that an extreme sensitivity to the presence of oxygen in the molecular system can be attained by increasing the anion-cation separation distance, and/or by removing the coordination interactions. Among the different molecular homologues studied in our previous work, compound **1** displays the greatest sensitivity to O_2 in the solid-state. We have previously demonstrated that in solution this complex can be converted into a mononuclear compound of Mn^{3+}, *via* a process of electron transfer between the complex and molecular oxygen. This reaction is characterized by a color change from colorless to intense violet. In contrast, when compound **1** is dispersed in DMF and irradiated at 360 nm, we do not observe appearance of any purple color characteristic of the photo-bleaching of the inserted complex. Furthermore, when **1** is illuminated in DMF solution in the presence of triphenylphosphine, the latter compound is rapidly converted to

triphenylphosphine oxide as followed by GCMS. These observations are in agreement with a production of singlet oxygen under light by compound **1**. Then, the compound **1** can be recovered by centrifugation and recycled for a new photo-reaction. The high sensitivity of compound **1** to oxygen could render it useful as a sensitizer, in oxygen sensing devices or in singlet oxygen generation reactions following type II photo-oxygenation mechanisms.

Conclusion

The strong luminescence, emitted at 600 nm (excitation at 360 nm) by the previously published tetra-nuclear clusters of Mn^{II} ions and two $ThiaSO_2$ macrocycles ($ThiaSO_2$ = *p-tert*-butylsulfonylcalixarene), of formula $[(ThiaSO_2)_2(Mn^{II})_4F]^-$, motivates us to try to define the full potential of this molecular system. In this context we were interested in the sensitivity of the luminescence emission of this system to oxygen. Previous work has led to the conclusion that the interaction of the cation with the anionic complex is of paramount importance. To exploit this phenomenon, we have carried out intercalation of the luminescent $[(ThiaSO_2)_2(Mn)_4F]^-$ anionic complex into the interlayer space of inorganic positively charged layers of layered double hydroxide (LDH) materials. Utilizing the osmotic swelling of layered double hydroxides (LDHs, $[Mg_{1-x}Al_x(OH)_2]^{x+}(NO_3^-)_x$) in formamide, the anionic luminescent $[(ThiaSO_2)_2(Mn^{II})_4F]^-$ complex has been introduced between the positive layers of LDHs, leading to a doping of LDH. In the recovered LDH layers the hexagonal prism morphology of the precursor is well retained. The formula of the resulting compound **1** ($Mg_{0.71}Al_{0.29}(OH)_2(NO_3)_{0.288}((ThiaSO_2)_2(Mn)_4F)_{0.002}(H_2O)_{0.5}$) was determined by elemental and thermogravimetric analysis. The low doping rate is attributed to the low negative charge density ($e/Å^2$) of the complex. Basal spacing of 12.02 Å indicates that $[(ThiaSO_2)_2(Mn)_4F]^-$ is sandwiched across the interlamellar width by positive LDH layers. The photophysical properties of the compound **1** were studied in the solid-state. Compound **1** presents

luminescence properties under UV excitation wavelength, with emission maxima centered at 630 nm under O_2 atmosphere. These photophysical studies have been carried out under different gaseous atmospheres using a range of excitation wavelengths. Extinction of emission in the presence of oxygen is reported, demonstrating the very high sensitivity of this compound to O_2. The LDH host matrix allows for the O_2-sensitivity to remain similar to that observed in solution whilst avoiding photo-degradation, thereby opening perspectives for use in oxygen sensing or singlet oxygen generation.

Experimental

Reagents and materials

All chemicals and solvents were used as received (solvents and chemicals: Aldrich). $[(ThiaSO_2)_2(Mn^{II})_4F]K$ compound was synthesized by the published procedure.[2a)]

Synthesis of $[Mg_2Al(OH)_6](CO_3)_{0.5}\cdot(3/2)H_2O$ *hydrotalcite (*Mg-Al-CO_3 LDH)

The LDH hydrotalcite is synthesized by a hydrothermal method. Four Teflon lined autoclaves each containing 12 cm^3 of an aqueous solution of $Mg(NO_3)_2\cdot 6H_2O$ (0.250 $mol.L^{-1}$), $Al(NO_3)_3\cdot 9H_2O$ (0.125 $mol.L^{-1}$) and hexamethylenetetramine (0.325 $mol.L^{-1}$) are heated to 150°C for 36 h. The resulting suspensions are collected together and centrifuged (8 500 rpm, 30 min) followed by subsequent washing in deionised water (3 x 25 cm^3) and ethanol (1 x 20 cm^3) with recovery by centrifugation each time. The product is dried overnight and recovered as a white microcrystalline powder (1.1428 g, 4.05 mmol with respect to formula, yield = 67%). P-XRD (2θ in °): 11.69, 23.54, 34.95, 35.64, 39.56, 47.07.

Synthesis of $[Mg_{0.72}Al_{0.28}(OH)_2](NO_3)_{0.28}(H_2O)_{0.36}$ *hydrotalcite (anion substitution: Mg-Al-*NO_3 *LDH)*

On a Schlenk line under Argon flow, Mg-Al-CO_3 LDH (0.3120 g, 1.11 mmol) is suspended in 150 cm^3 of a solution of $NaNO_3$ (1.0 $mol.L^{-1}$) and HNO_3 (5 mmol L^{-1}). This

mixture is agitated under Argon atmosphere at room temperature for 16 h, then is centrifuged (8 500 rpm, 30 min). The supernatant solution is decanted off and the solid material is washed with deionised water (3 x 50 cm^3) and 96% ethanol (1 x 40 cm^3). The product is dried under vacuum and recovered as a white microcrystalline powder (0.2650 g, 1.0 mmol, yield = 90% yield). P-XRD (2θ in °): 9.93, 19.95, 30.08, 34.74, 38.05, 40.47, 43.70. Formula was determined by TGA analysis and confirmed by elemental analysis (see Figure S1 in Supporting Information).

Synthesis of $[Mg_{0.71}Al_{0.29}(OH)_2](NO_3)_{0.288}((ThiaSO_2)_2(Mn)_4F)_{0.002}(H_2O)_{0.5}$ **1**: (*Intercalation of luminescent material)*

Many trials concerning variations of temperature, agitation, order of addition and so on were carried out for this reaction, to optimise the synthesis conditions as follows.

Under inert atmosphere (Ar) the nitrated form Mg-Al-NO_3 LDH (0.02 g, 0.24 mmol *i.e.* 0.067 mmol of NO_3^-) is added to formamide (50 cm^3) and allowed to form a homogenous dispersion such that the suspension becomes translucent and demonstrates Tyndall light scattering. 0.2 g (0.1 mmol) of $[(ThiaSO_2)_2(Mn)_4F]K$ dissolved in 4 cm^3 DMF is added dropwise to the solution of LDH with stirring. This mixture is agitated under inert atmosphere during 24 h. The suspension is then centrifuged (13 000 rpm, 5 min). The collected solid is washed with DMF (3 x 24 cm^3), degassed H_2O (3 x 24 cm^3) and ethanol (1 x 24 cm^3). The product **1** is dried at 50°C under reduced pressure, and collected as a pale yellow luminescent powder (0.019 g, yield = 88%)). P-XRD (2θ in °): 7.34°, 14.96° and 29.91. Elemental analysis (mass %): [Al] = 16.6%; [Mg] = 36.5%; [Mn] = 0.74%. Formula was supported by TGA analysis (see Figure S2 in Supporting Information).

Synthesis of $[Mg_{0.57}Al_{0.43}(OH)_2](NO_3)_{0.425}((ThiaSO_2)_2(Mn)_4F)_{0.005}$ **2**. The preparation of compound **2** is identical to compound **1** except for the stirring time, which is 72 hours. P-XRD

(2θ in °): 7.85°, 16.15° and 23.28. Elemental analysis (mass %): [Al] = 13.5%; [Mg] = 16.2%; [Mn] = 0.146%.

Characterizations

Scanning Electron Microscopy (SEM) was performed on a Vega Tescan SEM microscope. Elemental analysis was performed by ICP-OES (ICAP 6000 Thermo Fisher Scientific) for Al and Mg, and ICP-HRMS (ElementXR, Thermo Fisher Scientific) for trace Mn determination. Quantitative measurements were obtained after a wet acid digestion (HNO_3/HF mixture) of the powder.

Powder X-Ray Diffraction (P-XRD) was performed on a PANanlytical XpertPro MRD diffractometer with a Cu K$\alpha 1$ radiation (λ = 1.54060 Å) used with 40 kV and 30 mA settings in θ/θ mode, reflection geometry.

For Single Crystal X-Ray Diffraction (SC-XRD), suitable crystals were selected and mounted on an Xcalibur kappa geometry diffractometer (Rigaku OD, 2015) equipped with an Atlas CCD detector and using Mo radiation (λ = 0.71073 Å). Intensities were collected at 150 K by means of the CrysalisPro software.[17] Reflection indexing, unit cell parameters refinement, Lorentz polarisation correction, peak integration and background determination were carried out with the CrysalisPro software. An analytical absorption correction was applied using the modelled faces of the crystal.[18] The structures were solved by direct methods with SIR97 and the least square refinement on F^2 was achieved with the Crystalis software. All non-hydrogen atoms were refined anisotropically. The hydrogen atoms were all located in a difference map, but those attached to carbon atoms were repositioned geometrically. The H atoms were initially refined with soft restraints on the bond lengths and angles to regularize their geometry (C-H in the range 0.93 - 0.98 Å, and U_{iso}(H) in the range 1.2 - 1.5 times U_{eq} of the parent atom), after which the positions were refined with riding constraints. For the experimental details see Supporting Information. CCDC-2010107 contains the supplementary crystallographic data for

this paper. These may be obtained free of charge from The Cambridge Crystallographic Data Centre via www.ccdc.cam.ac.uk/data_request/cif. Spectroscopic measurements.

Solid-state excitation and emission spectra were recorded with a commercial fluorimeter Fluorolog 3 from Horiba Jobin Yvon Co, equipped with a Xe lamp 450 W, and a UV-visible photomultiplier (Hamamatsu R928, sensitivity 185 - 900 nm). The excitation/emission spectra were realized on powder samples pasted directly onto copper plates using conductive silver glue. For the measurements realized at variable temperature (77 K – 300 K), the samples were introduced into an OptistatCF liquid nitrogen cooled cryostat from Oxford Instruments Co. The emission spectra were corrected for the instrumental response function. Appropriate filters were utilized to remove the laser light, the Rayleigh scattered light and associated harmonics from the emission spectra. Luminescence lifetime ($\tau > 10$ μs) have also been measured using this apparatus with a xenon flash lamp (phosphorescence mode) Lifetimes were averages of 2 or 3 independent determinations. The air pressure dependent solid-state luminescence spectra have been realized in a cryostat equipped with a primary pump.

For illumination experiments, LEDs of various wavelengths 360 and 400 nm were used. The LED were purchased from LED ENGINE Co and calibrated with a flame spectrometer from Ocean Optic with a nominal flux of 430 and 586 mW/cm^2, respectively, at a working distance between the source and the sample of d = 10 mm.

---

[1] P. Gomez-Romero, C. Sanchez, Functional hybrid materials Wiley-VCH, 2004.

[2] a) M. Lamouchi, E. Jeanneau, A. Pillonnet, A. Brioude, M. Martini, O. Stéphan, F. Meganem, G. Novitchi, D.Luneau and C. Desroches, Dalton Trans., 2012, 41, 2707. b) Y. Suffren, N. O'Toole, A. Hauser, E. Jeanneau, A. Brioude and C. Desroches, Dalton Trans., 2015, 44, 7991 c) N. O'Toole, C. Lecourt, Y. Suffren, A. Hauser, L. Khrouz, E. Jeanneau, A. Brioude, D. Luneau and C. Desroches, Eur. J. Inorg. Chem., 2019, 73.

[3] V. Rives, Layered double hydroxides present and future, Nova Science Publishers, Inc. 2001.

[4] D. Xue, D. G. Evans, Layered Double Hydroxides, Springer Science & Business Media, 2006.
[5] D. P. Yan, J. Lu, M. Wei, D. G. Evans, X. Duan, J. Mater. Chem., 2011, 21, 13128.
[6] (a) T. Hibino, Chem. Mater., 2004, 16, 5482; (b) G. L. Huang, S. L. Ma, X. H. Zhao, X. J. Yang, K. T. Ooi, Chem. Comm., 2009, 3, 331.
[7] K. Okamoto, N. Iyi,; T. Sasaki, Appl. Clay Sci., 2007,37, 23.
[8] R. Z. Ma, T. Sasaki, Adv. Mater., 2010, 22, 5082.
[9] K. L. Xu, G. M. Chen, J. Q. Shen, Rsc Adv., 2014, 4, 8686.
[10] Z. P. Xu, H. C. Zeng, J. Phys. Chem. B, 2001, 105, 1743.
[11] a)S. Satoru, A. Sumio, H. Hidetoshi, S. Akira, N. Eiichi, Chem. Lett., 2004, 33, 790. b) S. Satoru, A. Sumio, H. Hidetoshi, S. Akira, H. Nakayama, N. Eiichi, J. Solid State Chem., 2006, 179, 1129.
[12] G. Huang, S. Ma, X. Zhao, X. Yang, K. Ooi, Chem. Mater., 2010, 22, 1870
[13] E. P. Giannelis, D. G. Nocera, T. J. Pinnavaia, Inorg. Chem., 1987, 26, 203.
[14]K. Nejati, A. Mokhtari, F. Khodam, Z. Rezvani, Can. J. Chem., 2016, 94, 66.
[15] S. Miyata, Clays Clay Miner., 1975, 23, 369.
[16] M. Veith, M. Jarczyk, V. Huch, Angew. Chem. Int. Ed., 1998, 37, 105.
[17] Rigaku Oxford Diffraction, 2018, CrysAlisPro Software system, version 1.171., Rigaku Corporation, Oxford, UK.
[18] R. C. Clark, and J. S. Reid, 51 Acta Cryst. A, 1995, 887.